

FEM PROGRESSIVE FAILURE SIMULATION OF REINFORCED CONCRETE MEMBERS ON SHEAR

Viktor HRISTOVSKI*¹ and Hiroshi NOGUCHI*²

ABSTRACT: Application of a smeared, rotating-crack hypo-elastic model for progressive failure analysis of reinforced concrete members subjected to lateral forces has been discussed. Two approaches have been applied: the first one, taking into account only the normal crack mode (*basic model*), and the second approach, based on the first one, however with included shear-slip mechanism along crack surfaces (*integral model*). Using originally developed software for non-linear analysis of reinforced concrete structures, as well as the characteristic specimens recommended by Japan Concrete Institute for model verification, a good agreement between analytical and experimental results has been obtained.

KEYWORDS: hypo-elastic model, finite element analysis, shear-slip mechanism, rotating cracks, smeared approach, progressive failure analysis

1. INTRODUCTION

The principal objective of this research is development of 2D reinforced concrete material constitutive models, which take into account the specific cracking phenomena that significantly contribute to the non-linear behavior of the RC members subjected to lateral forces. The models are based on the rate-independent hypo-elastic approach with smeared rotating cracks, according to Noguchi [1], leading to the assumption of identical directions of the material axes with the axes of the principal stresses. However, since this excludes participation of shear stresses in the crack planes, a concept based on the Vecchio's physical model [7] taking into account the local shear stresses along the crack planes and the shear-slip relation proposed by Walraven [2], has been herein adopted. The reinforcement bars have been treated by bi-linear elastic-plastic mixed-hardening model for both discrete and smeared definitions, also assuming perfect bond between bars and concrete.

2. CONSTITUTIVE RELATIONS

The basic idea of the proposed models is to treat the biaxial state of stresses and strains of concrete by uniaxial constitutive relations in principal directions 1 and 2, using the *equivalent uniaxial strain functions*. The principal stresses and strains are allowed to rotate in coaxial directions during the loading process, satisfying the form invariance condition. However, in the cases where a large rotation is expected (as in the analysis of beam-column joints), control of this rotation becomes necessary in order to prevent numerical instabilities during calculation. Therefore, the improved accuracy is provided by transformation of the principal axes in case when the rotation relating to the original state becomes greater than 45 degrees, in such a way that the stresses, strains and stiffness regarding the axis 1 are substituted to the corresponding quantities related to axis 2, and vice versa (Noguchi [1]).

The stress-update scheme is based on the hypo-elastic incremental formulation, where the "predictor" stresses in each integration point of the finite elements can be calculated as follows:

*1 Dept. of Design & Arch., Faculty of Engineering, Chiba University, Post-doctoral Researcher from Macedonia (Institute of Earthquake Engineering and Engineering Seismology, Skopje)

*2 Dept. of Design & Arch., Faculty of Engineering, Chiba University, Professor, Member of JCI

$$\boldsymbol{\sigma}_{n+1} = \boldsymbol{\sigma}_n + d\boldsymbol{\sigma}_{n+1} \quad (1)$$

$$d\boldsymbol{\sigma}_{n+1} = \mathbf{C}_T d\boldsymbol{\varepsilon}_{n+1} \quad (2)$$

In Eqs. (1) and (2), $\boldsymbol{\sigma}_n$ and $\boldsymbol{\sigma}_{n+1}$ are stress vectors from previous and actual load step, respectively; $d\boldsymbol{\sigma}_{n+1}$ and $d\boldsymbol{\varepsilon}_{n+1}$ are actual incremental stresses and strains, while \mathbf{C}_T is the matrix of *elastic tangent material moduli* in global coordinate system, which depends on the previous state of the equivalent uniaxial strain functions ε_u . According to Noguchi [1], the increments of these functions $d\varepsilon_u$ can be related to the increments of the strains in principal directions $d\varepsilon_p$ using the following equation (with ν being Poisson's ratio):

$$d\boldsymbol{\varepsilon}_u = \frac{1}{1-\nu^2} \begin{bmatrix} 1 & \nu \\ \nu & 1 \end{bmatrix} d\boldsymbol{\varepsilon}_p \quad (3)$$

Hence the new total equivalent strains can be obtained from the relation:

$$\boldsymbol{\varepsilon}_{u,n+1} = \boldsymbol{\varepsilon}_{u,n} + d\boldsymbol{\varepsilon}_u \quad (4)$$

In Eq. (4), $\boldsymbol{\varepsilon}_{u,n+1}$ and $\boldsymbol{\varepsilon}_{u,n}$ are the total equivalent strain functions for previous and current load steps, respectively.

The *failure functions* adopted in the model are based on the Kupfer's [3] yield curve for bi-axial stresses, taking into account the influence of the strength reduction of cracked concrete in compression, according to Noguchi [4]. Hence, particularly, for the combination of stresses "tension-compression", when tension strain is greater than cracking strain, the following expressions are used:

$$\sigma_{c2} = \frac{f_c}{0.27 + 0.96 \left(\frac{\varepsilon_{u1}}{\varepsilon_{cu}} \right)^{0.167}} \geq f_c \quad (5a)$$

$$\sigma_{c1} = \sigma_{c2} \quad (5b)$$

In Eqs. (5a) and (5b), σ_{c1} and σ_{c2} are failure stresses in principal directions, $f_c < 0$ is uniaxial concrete strength in compression, $\varepsilon_{u1} > 0$ and $\varepsilon_{cu} < 0$ are equivalent uniaxial strain function in principal direction 1 (in tension) and uniaxial strain in compression for the corresponding strength f_c , respectively.

Once the equivalent uniaxial strains have been calculated using the Eq. (4), the corresponding *equivalent uniaxial stresses* σ_{u1} and σ_{u2} in principal directions can be found by the Saenz's [5] *uniaxial relation for compression* (Eq.(6)):

$$\sigma_{u2} = \frac{E_o \varepsilon_{u2}}{1 + \left(E_o \frac{\varepsilon_{c2}}{\sigma_{c2}} - 2 \right) \frac{\varepsilon_{u2}}{\varepsilon_{c2}} + \left(\frac{\varepsilon_{u2}}{\varepsilon_{c2}} \right)^2} \quad (6)$$

or by *tension-stiffening function* proposed by Shirai[6] (Eqs. (7a), (7b)):

$$\sigma_{u1} = f_t (1 - 2.748\xi + 2.654\xi^2 - 0.906\xi^3) \quad (7a)$$

$$\xi = \frac{\varepsilon_{u1} - \varepsilon_{cr}}{\varepsilon_m - \varepsilon_{cr}} \quad (7b)$$

depending on the stress-strain states. In Eqs. (7a) and (7b) E_o is the initial concrete modulus of elasticity, f_t

is the concrete tension strength, ε_{cr} is a concrete cracking strain and ε_m is a tension strain for zero stresses. In the analyses, the constitutive parameters according to **Fig. 1** have been adopted ($i=1, 2$). Once σ_{u1} and σ_{u2} have been found, the corrected total stress vector σ_{n+1} can be calculated by using transformation from local (principal) into global coordinate system.

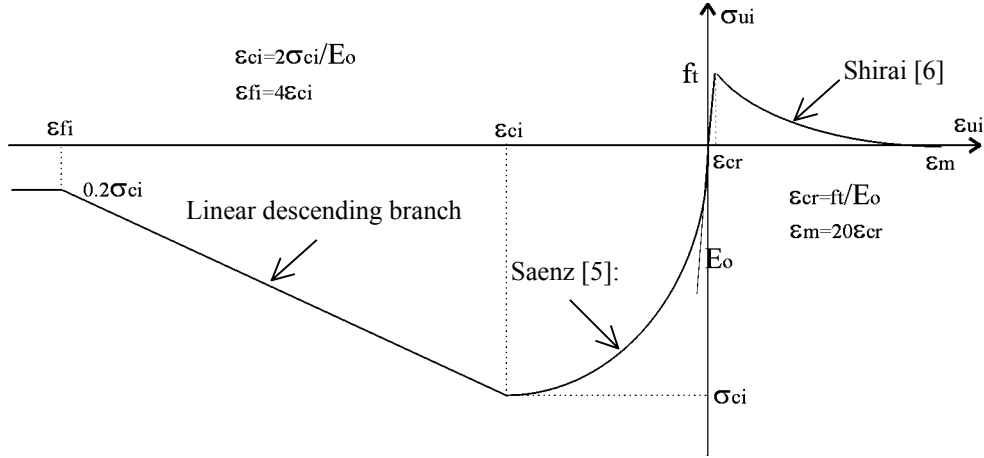


Fig. 1 Adopted constitutive relations for concrete

For cases where the shear-slip phenomenon plays significant role during the progressive failure process (especially for behavior of shear walls), a *smearred shear-slip approach* based on the physical model published recently by Vecchio (Disturbed Stress Field Model [7]), however, by using the incremental-load, tangent-stiffness formulation, is herein proposed. The approach is based on the stiffness portion of Walraven's shear-slip relationship for the cracked surfaces [2], as follows:

$$\delta = \frac{\tau_c}{1.8w^{-0.8} + (0.234w^{-0.707} - 0.2)f_{cc}} \quad (8)$$

In Eq. (8) δ is tangential slip along the crack, w is crack width, f_{cc} is cube concrete compressive strength and τ_c is *local shear stress* acting on the crack. Actually, according to the Vecchio's physical model, local stress variations of the reinforcement bars crossing the crack, as well as the local stresses of the concrete between the cracks induce *local shear stress* (the average shear stress in the integration point remains equal to zero). Satisfying the equilibrium conditions along the crack surface (**Fig. 2**), this local shear stress can be calculated, as follows:

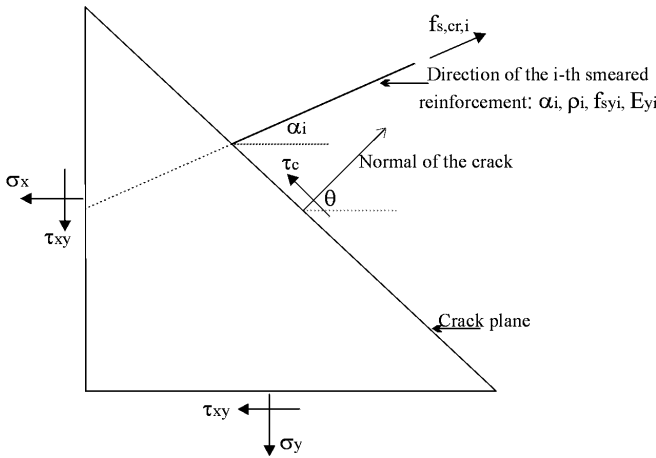


Fig. 2 Local equilibrium conditions along the crack surface resulting in local shear stress τ_c and shear-slip δ

$$\tau_c = \sum_{i=1}^n \rho_i (f_{s,cr,i} - f_{s,i}) \cos \theta_i \sin \theta_i \quad (9)$$

In Eq. (9), ρ_i is the reinforcement ratio of the i -th reinforcement (with the direction α_i related to the global x -axis) crossing the crack, while θ_i is the difference between angle of the principal direction 1 and angle of the reinforcement direction α_i . Functions $f_{s,cr,i}$ and $f_{s,i}$ are local steel stress (at the analyzed crack) and the average steel stress in the integration point of the actual finite element, respectively. Although this shear stress is only local, it results in slippage δ along the crack, which can be estimated using the Eq. (8). In this equation, the frictional properties of

the crack surfaces (aggregate-interlock) are already taken into account. The idea of the proposed numerical approach is to calculate the incremental slip strains $d\epsilon_{slip}$ from the slippage δ and consequently the *additional unbalanced stresses* $d\sigma_{slip}$ induced by these strains, as follows:

$$d\sigma_{slip} = C_T d\epsilon_{slip} \quad (10)$$

The proposed *integral algorithm* can be used only for the smeared formulation of the reinforcement, providing stable numerical consistency especially for the cases of RC members with reinforcement in both directions, having approximately the same reinforcement ratio (as in case of shear walls).

3. NUMERICAL VERIFICATION

Verification of the both models (*basic* one – based on the definition without shear-slip influence and *integral* one – based on smeared steel definition and shear-slip relation) has been done using the results from experiments conducted on samples recommended for model verification by Japan Concrete Institute

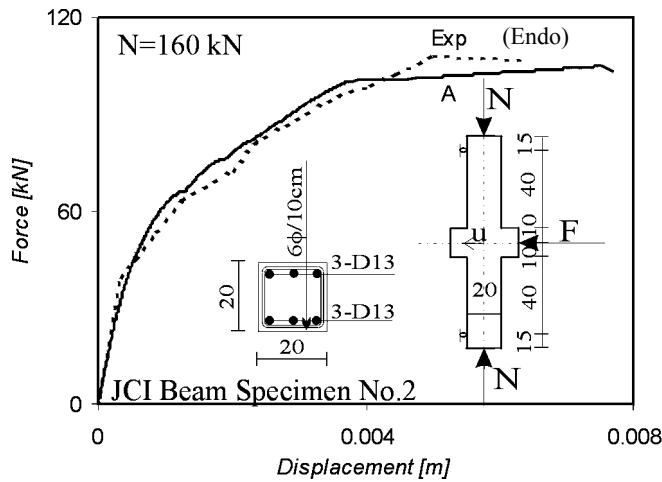


Fig. 3 Geometry of the JCI Specimen No. 2 and comparison of the obtained P-Delta diagrams, experimentally (Exp) and analytically (A)

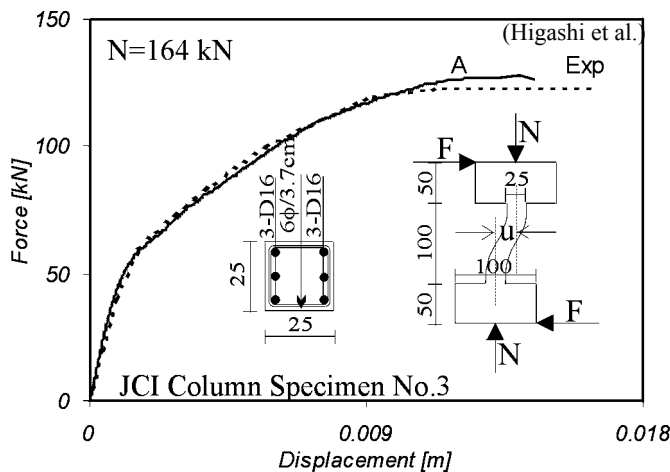


Fig. 4 Geometry of the JCI Specimen No. 3 and comparison of the obtained P-Delta diagrams, experimentally (Exp) and analytically (A)

Tab. 1. Material properties for the JCI Beam Specimen No.2

Concrete:		Steel:	
f'_c [MPa]	18.4	f_y [MPa]	E_s [GPa]
E_c [GPa]	21.4	D13	473
f'_t [MPa]	2.04	6φ	333

f'_c – Uniaxial compressive concrete strength

E_c – Initial concrete modulus of elasticity

f'_t – Uniaxial tensile concrete strength

f_y – Yielding stress of reinforcement

E_s – Initial modulus of elasticity of reinforcement

Tab. 2. Material properties for the JCI Column Specimen No.3

Concrete:		Steel:	
f'_c [MPa]	24.0	f_y [MPa]	E_s [GPa]
E_c [GPa]	23.0	D16	395
f'_t [MPa]	1.68	6φ	454.6

(JCI) [8]. Within this paper, one beam and one column specimens have been considered using the basic model, and two shear-walls have been treated using the integral approach. Applied finite element analytical models, consisting of meshes with 8 and 9 node iso-parametric serendipity elements for concrete (including smeared steel) and truss elements for discrete bars, are more detailed explained in **Tab. 4**, together with the details about the experimentally observed failure modes and comparison of the analytical and experimental shear capacities. It should be noted that the experiments were conducted on cyclic loading. The materials

properties of the specimens are given in **Tabs. 1, 2 and 3**, and the results of the analyses (via force-displacement diagrams) are given in **Figs. 3, 4, 5 and 6**, where analyses denoted by “A1” correspond

Tab. 3. Material properties of the JCI Shear-Wall Specimens #1 and #1'' used in analyses

CONCRETE		STEEL					
		Columns t=20 cm		Beams t=30 cm		Wall t=10 cm	
		Diameter	f_y [MPa]	Diameter	f_y [MPa]	Diameter	f_y [MPa]
f_c' [MPa]	29.7	D13	368	D10	353	6 ϕ (2x6 ϕ /7.5 cm, vert. and horiz.)	363
E_c [GPa]	23.4	6 ϕ	399	D22, D29	400 (default)		
f_t' [MPa]	2.36						

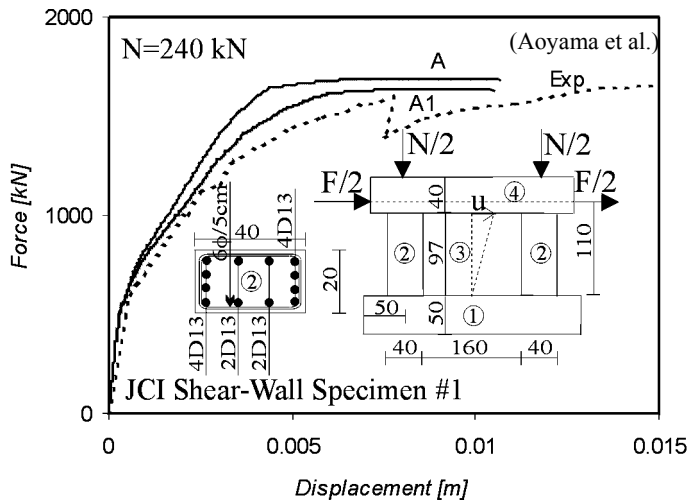


Fig. 5 Geometry of the JCI Specimen #1 and comparison of the obtained P-Delta diagrams, experimentally (Exp) and analytically (A and A1)

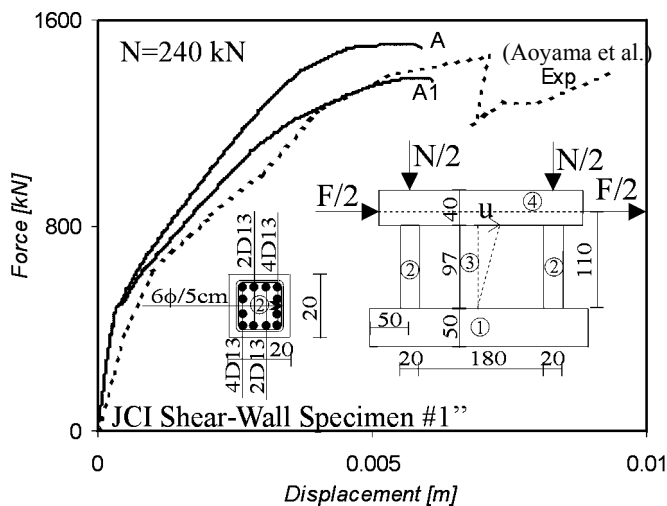


Fig. 6 Geometry of the JCI Specimen #1'' and comparison of the obtained P-Delta diagrams, experimentally (Exp) and analytically (A and A1)

to the integral algorithm, and the analyses "A" are related to the basic one. The numerical solution has been performed using the incremental-iterative Newton-Raphson algorithm, based on the force and displacement-control scheme. It should be noted that the analytical results up to the peak capacities have been here treated as physically meaningful (as they have been presented), although the computations have continued further following the descending branch of the force-displacement diagrams.

4. CONCLUSIONS

Although, using the both described hypo-elastic constitutive models for concrete and elastic-plastic model for steel, correct simulations of the experimental behavior have been achieved not only regarding the force-displacement diagrams, but also with respect to the obtained failure mechanisms and crack patterns (see Fig. 7: comparison of the analytically and experimentally obtained crack patterns after the first half-cycle for shear wall #1), several remarks should be drawn regarding the models limitations. The greater analytically obtained ductility and less capacity compared to experimental ones for spec. No. 2 (analyzed by basic model) have shown that the modeling of the shear-transfer for members failed on shear-tension (ST) could

be important. However, as to the specimen No.3, since the capacity at splitting-bond was experimentally found to be about 84 % of the maximum shear force, the discrepancy between analysis and experiment has not been so emphasized, in spite of the fact that the bond properties between steel and concrete have not been modeled in the analysis. The integral model has shown to be crucial for more correct simulation of the failure progress for shear walls and members with predominant shear behavior, especially where the slippage along the cracks in the walls (SSC) are recognized as one of the failure modes (see Tab. 4 for SW specimens #1 and #1''). However, discrepancy in P-Delta diagrams regarding the displacements still exists, probably due to the experimentally observed slip on the boundaries between the parts with different thickness (failure mode SSB) that has not been considered in the model.

ACKNOWLEDGMENTS

The authors would like to express their appreciations to the Japan Society for the Promotion of Science (JSPS) that supported this research through the Post-doctoral Fellowship Program for Foreign Researchers. Also, by the courtesy of the Japan Concrete Institute (JCI), the authors appreciate the opportunity of using the selected and recommended specimens for model verification.

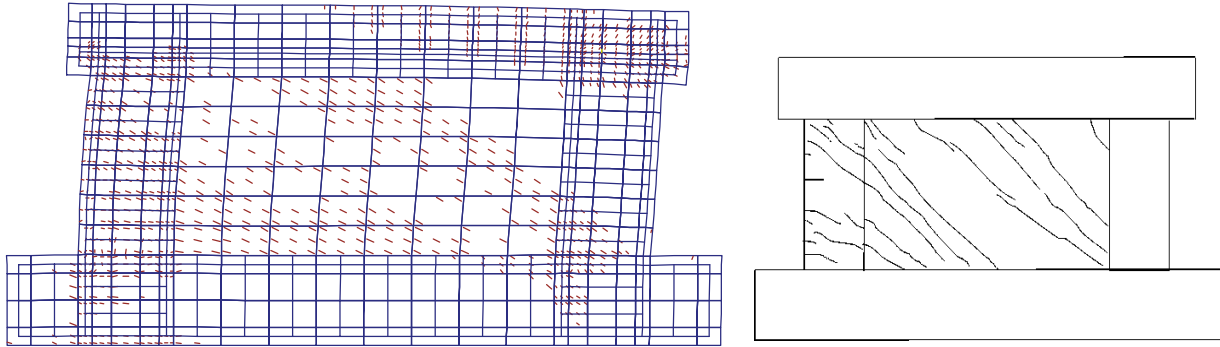


Fig. 7 Obtained crack patterns after the first half-cycle (SW#1): left - analytically, right - experimentally

Tab. 4 Finite element mesh characteristics, obtained shear capacities and failure modes

Specimen	Applied FE for concrete	Applied FE for steel bars		Shear capacity (kN)		FM (Exper.)
		Beams & Columns	Wall	Exper.	Anal.	
JCI beam No.2	56 IP with 8-nodes	Discrete: 62 T		108	105	F, ST
JCI column No.3	92 IP with 8 (9) nodes	Discrete: 254 T		123	128	F, C, Bo
JCI shear wall #1	296 IP with 8 (9) nodes	Discrete: 1198 T	Smearred	1650	1638	C, SSB, SSC
JCI shear wall #1”	306 IP with 8 (9) nodes	Discrete: 1135 T	Smearred	1410	1378	C, SC, SSB, SSC

IP – Isoparametric finite elements for plane-stress with 3x3 Gaussian integration rule, T – Truss elements
 FM (Failure modes): F – Flexural (yielding of tensile reinforcing bar), C – Crush of concrete in column, Bo – Splitting bond, ST – Shear tension, SC-Shear compression in wall, SSC – Failure due to shear slip along cracks in wall, SSB – Fail. due to shear slip of wall along the bottom beam

REFERENCES

1. Noguchi, H. “Analytical Models for Reinforced Concrete Members Subjected to Reversed Cyclic Loading,” Proc., Seminar on Finite Element Analysis of Reinforced Concrete Structures, Volume 2, JSPS, Tokyo, May 21-24, 1985, pp.93-112
2. Walraven, J.C., “Fundamental Analysis of Aggregate Interlock,” ASCE Journ. of Structural Engineering, Vol.107, No.11, 1981, pp.2245-2270
3. Kupfer, H. and Gerstle, K. H., “Behavior of Concrete under Biaxial Stresses,” ASCE Journal of Engineering Mechanics Division, Vol.99, No.EM4, Proc. Paper 9917, Aug. 1973, pp.852-866
4. Noguchi, H., Ohkubo, M. and Hamada S., “Basic Experiments on the Degradation of Cracked Concrete under Biaxial Tension and Compression,” Proc. of JCI, Vol.11, No.2, 1989, pp.323-326 (In Japanese)
5. Saenz, L.P., “Discussion of “Equation for the Stress-Strain Curve of Concrete” by Desayi and Krishnan,” ACI Journal, Vol.61, September 1964, pp. 1229-1235
6. Shirai, N. and Sato, T., ‘Bond-Cracking Model for Reinforced Concrete,’ Trans. of the JCI, Vol. 6, 1984
7. Vecchio, F. J., “Disturbed Stress Field Model for Reinforced Concrete: Formulation,” Journal of Structural Engineering, ASCE, Vol. 126, No. 9, September, 2000, pp. 1070-1077
8. JCI, “Collected Experimental Data of Specimens for Verification of Analytical Models,” Proceedings of JCI 2nd Colloquium on Shear Analysis of RC Structures, JCI-C6, October 1983, pp.9-20, 43-54 (In Japanese)